

Water-based Fe_2O_3 Ferrofluid Flow over a Rotatable Plate

ANUPAM BHANDARI*, AKMAL HUSAIN

Department of Mathematics,
School of Advanced Engineering,
University of Petroleum and Energy Studies (UPES), Dehradun,
Energy Acres Building, Bidholi,
Dehradun- 248007, Uttarakhand,
INDIA

Abstract: - In the current work, the influence of rotational viscosity as a result of an external magnetic field on water-based Fe_2O_3 ferrofluid flow over a rotating plate is investigated. The governing equations of the physical model are transformed into a set of ordinary differential equations. The numerical solution of the differential equations is obtained by using the finite element method. The findings of the radial, tangential, and axial velocity distributions are descriptively presented for the different range of rotational viscosity. The outcomes of this research demonstrate that the magnetic field has an important role in controlling the velocity profiles in the flow. A comparative study of velocity distributions is presented for COFe_2O_4 , Fe_2O_3 , NiO, and CO nanoparticles.

Key-Words: - Ferrofluid; rotating disk; velocity; magnetic field; rotational viscosity; differential equations.

Received: January 7, 2023. Revised: November 13, 2023. Accepted: December 11, 2023. Published: December 31, 2023.

1 Introduction

Ferrofluids are smart materials that can vary their rheological and physical characteristics for the sake of the external magnetic field. Ferrofluids are colloidal suspensions of single-domain magnetic nanoparticles (3-15nm approx.), [1], [2], [3]. It is composed of iron oxide ($\gamma - \text{Fe}_2\text{O}_3$, Fe_3O_4), MnZn ferrites, Ni, Fe, and CO in carrier liquid after adding some surfactant to avoid the agglomeration of nanoparticles, [4], [5], [6]. Because of the nanosize of the particles, ferrofluids contribute significantly to nanoscience and nanotechnology. Ferrofluids can achieve a broad range of viscosity subject to the availability of a magnetic field. Ferrofluids are generally needed in the sealing of hard disks, electronic packaging, aerospace engineering, loudspeaker coils, and biomedical engineering, [7]. Ferrofluids manifest rotational viscosity and the origin of the additional viscosity becomes due to the difference between the speed of the rotation of the nanoparticles and fluid vorticity. The medical implementation such as drug targeting and hyperthermia are gaining considerable attention, [8], [9], [10]. [11], used the Keller-box approach to solve the similarity differential equations while studying the magnetohydrodynamic flow and heat transport over a shrinking surface. [12], investigated how thermal radiation affected magnetohydrodynamic flow over a sheet that

was stretching exponentially and came up with a numerical solution using the shooting method. [13], measured the effects of activation energy and sheet thickness variation by examining the rotational hydromagnetic flow of Carreau fluid. The flow behavior of magnetic fluid has attracted many researchers due to its diversified applications. Attia has studied MHD flow near a rotating disk with various parameters, [14], [15], [16], [17]. The researchers have examined the rheological characteristics of ferrofluid, [18], [19]. In a magnetic fluid, [1], introduced magneto-viscous phenomena. An important aspect of rotational viscosity due to the magnetic field named known as negative viscosity has been explained in detail, [20]. Using a few new mathematical expressions, [21], provides a theoretical explanation of negative viscosity. [22], presented a novel magnetization equation. [23], investigated the flow of nanofluids in a vertical plate. The influence of magnetization force and viscosity in ferrofluid flow in the presence of a disk has been investigated, [24], [25], [26], [27]. Under the influence of a strongly oscillating magnetic field, the ferrofluid generated by a stretchy rotating plate was examined, [28]. [29], investigated the effects of rotational viscosity in water-based ferrofluid through experimental work. [30], analyzed the pipe flow of magnetic fluid in an oscillating magnetic field with variable viscosity.

[31], investigated microstructure and inertial characteristics in ferrofluid flow over a stretching sheet. Different classes of nanofluid flow and heat transfer properties have been studied by researchers, [32], [33], [34], [35], [36].

In the present work, the influence of rotational viscosity on the steady and incompressible flow of Fe_3O_4 as a result of a rotating plate has been investigated. The magnetization equation derived by Shliomis from irreversible thermodynamics has been employed to calculate an increase of the ferrofluid viscosity in the presence of an oscillating magnetic field. In response to the magnetic field, fluid, and magnetic nano-particles rotate with different angular velocities, which creates an additional resistance on the velocity distribution. Similarity transformation has been used to transform a set of differential equations in dimensionless form. The shooting method has been used to solve a system of nonlinear-coupled differential equations. This resistance to the velocity profiles for different values of field-dependent viscosity parameters has been investigated.

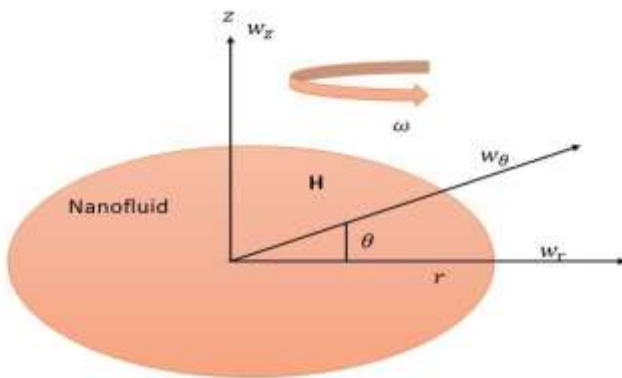


Fig. 1: Flow configuration of nanofluid flow over a rotatable plate

2 Problem Formulation

Figure 1 shows the flow configuration for the nanofluid. The plate rotates with a uniform angular velocity about z axis. The components of the radial, tangential, and axial velocity distributions are w_r , w_θ and w_z , respectively. The disk is kept in a uniform magnetic field which is balanced by the pressure gradient. The governing equations for the ferrohydrodynamic nanofluid flow are as follows:

$$\rho_n \left(\frac{\partial}{\partial t} + \mathbf{w} \cdot \nabla \right) \mathbf{w} = -\nabla p + \mu_n \nabla^2 \mathbf{w} + \mu_0 (\mathbf{M} \cdot \nabla) \mathbf{H} + \frac{I}{2\tau_s} \nabla \times (\boldsymbol{\omega}_n - \boldsymbol{\Omega}), \quad (1)$$

$$\frac{d\mathbf{M}}{dt} = \boldsymbol{\omega}_n \times \mathbf{M} - \frac{1}{\tau_B} (\mathbf{M} - \mathbf{M}_0), \quad (2)$$

$$I \frac{d\boldsymbol{\omega}_n}{dt} = \mathbf{M} \times \mathbf{H} - \frac{I}{\tau_s} (\boldsymbol{\omega}_n - \boldsymbol{\Omega}), \quad (3)$$

$$\nabla \cdot \mathbf{w} = 0, \quad (4)$$

where ρ_n exhibits the density, \mathbf{w} indicates the fluid velocity, p represents the pressure, μ_n exhibits the reference viscosity, μ_0 exhibits the magnetic permeability of free space, \mathbf{M} exhibits the magnetization, \mathbf{H} represents the magnetic field intensity, $\boldsymbol{\omega}_n$ indicates the angular velocity of the particle, $\boldsymbol{\Omega}$ indicates the vorticity of the flow, t indicate the time, τ_s indicates the Neel relaxation time and I indicates the sum of the particle moment of inertia.

Instantaneous equilibrium Magnetization \mathbf{M}_0 is defined in terms of Langevin function as:

$$\mathbf{M}_0 = nmL(\xi) \frac{\mathbf{H}}{H}, \quad \xi = \frac{mH}{kT}, \quad L(\xi) = \coth \xi - \xi^{-1}, \quad (5)$$

where τ_B indicates the Brownian relaxation time, m indicates the magnetic moment of the particle, ξ indicates the Langevin parameter, k indicates the Boltzmann constant and T indicates the temperature. Considering $I \frac{d\boldsymbol{\omega}_n}{dt} \ll I \frac{\boldsymbol{\omega}_n}{\tau_s}$, Eq. (3) can be expressed as:

$$\boldsymbol{\omega}_n = \boldsymbol{\Omega} + \frac{\tau_s}{I} (\mathbf{M} \times \mathbf{H}) \quad (6)$$

Eq. (6) reduces Eq.(1)-(2) as:

$$\rho_n \left(\frac{\partial}{\partial t} + \mathbf{w} \cdot \nabla \right) \mathbf{w} = -\nabla p + \mu_0 (\mathbf{M} \cdot \nabla) \mathbf{H} + \mu_n \nabla^2 \mathbf{w} + \frac{1}{2} \nabla \times (\mathbf{M} \times \mathbf{H}) \quad (7)$$

$$\frac{d\mathbf{M}}{dt} = \boldsymbol{\Omega} \times \mathbf{M} - \frac{1}{\tau_B} (\mathbf{M} - \mathbf{M}_0) - \frac{\tau_s}{I} \mathbf{M} \times (\mathbf{M} \times \mathbf{H}) \quad (8)$$

Where $\tau_B = \frac{3\mu_n V}{kT}$ is called Brownian relaxation time. Using Eq. (6), the equilibrium of magnetic and viscous torque can be presented as:

$$\mathbf{M} \times \mathbf{H} = -6\mu_n \varphi (\boldsymbol{\Omega} - \boldsymbol{\omega}_n) \quad (9)$$

Where φ denotes the volume concentration. The non-equilibrium actual magnetization is considered to be the equilibrium as:

$$\mathbf{M} = \frac{\varphi M_s L(\xi_e) \xi_e}{\xi} \quad (10)$$

Where ξ_e indicates the effective magnetic field parameter and $L(\xi)$ denotes the Langevin function. The effective magnetic parameter is a ratio of effective magnetic force and thermal force i.e. $\xi_e = \frac{mH_e}{kT}$. Owing to the slow and oscillating magnetic field, Eq. (8) can be written as, [17], [18]:

$$\frac{d}{dt} \left(L_e \frac{\xi_e}{\xi} \right) = \boldsymbol{\Omega} \times \left(L_e \frac{\xi_e}{\xi} \right) - \frac{1}{\tau_B} \frac{L_e}{\xi_e} (\xi_e - \xi) - \frac{L_e^2}{2\tau_B \xi_e^2} (\xi_e \times \xi_e \times \xi) \quad (11)$$

The effective field parameter by the equation of zero approximation from Eq. (11) as, [21]:

$$\tau_B \frac{d\xi_e}{dt} = - \left(\frac{d \ln L_e}{d \xi_e} \right) \left(1 - \frac{\xi_0}{\xi_e} \cos \omega_0 t \right), \quad (12)$$

ξ_0 is the amplitude of the magnetic field. The linear approximations in $\Omega \tau_B$, Eq. (11) gives $M = M_0 R(\xi_e) \tau_B \boldsymbol{\Omega} \times \mathbf{h}$ where $M_0 = nmL(\xi)$ and \mathbf{h} is a unit vector, [21]. Then the function $R(\xi_e)$ is determined by Eq. (11) as:

$$\tau_B \frac{dR}{dt} = 1 - \frac{1}{2} \left(\frac{1}{L_e} - \frac{1}{\xi_e} \right) \xi_0 R \cos \omega_0 t, \quad (13)$$

where $R(\xi_e)$ denotes the effective magnetization function and ω_0 denotes the angular frequency of the magnetic field.

The mean magnetic torque is as:

$$\overline{\mathbf{M} \times \mathbf{H}} = -6\mu_n \varphi \sigma \boldsymbol{\Omega}, \quad \sigma = \frac{1}{2} \xi_0 \overline{\cos \omega_0 t L(\xi_e) R(\xi_e)} \quad (14)$$

$$\begin{aligned} \frac{1}{2} \nabla \times \overline{\mathbf{M} \times \mathbf{H}} &= \frac{1}{2} \nabla \times -6\mu_n \varphi \sigma \boldsymbol{\Omega} \\ &= -\frac{3}{2} \mu_n \varphi \sigma \nabla (\nabla \cdot \mathbf{w}) + \frac{3}{2} \mu_n \varphi \sigma \nabla^2 \mathbf{w} \\ &= \frac{3}{2} \mu_n \varphi \sigma \nabla^2 \mathbf{w} \end{aligned} \quad (15)$$

Thus $\Delta \mu = \frac{3}{2} \mu_n \varphi \sigma$ the magnetic field-dependent viscosity and the angular velocity of the nanoparticle may be expressed $\boldsymbol{\omega}_n = (1 - \sigma) \boldsymbol{\Omega}$, [21]. Eq. (1) can be written with the help of Eq. (15) as:

$$\rho_n \left(\frac{\partial}{\partial t} + \mathbf{w} \cdot \nabla \right) \mathbf{w} = -\nabla p + \mu_0 (\mathbf{M} \cdot \nabla) \mathbf{H} + \mu_n \left(1 + \frac{3}{2} \varphi \sigma \right) \nabla^2 \mathbf{w} \quad (16)$$

Magnetization force and pressure force can be merged as:

$$-\nabla \tilde{p} = -\nabla p + (\mathbf{M} \cdot \nabla) \mathbf{H} \quad (17)$$

The momentum equation can be expressed in the reduced pressure form as:

$$\rho_n \left(\frac{\partial}{\partial t} + \mathbf{w} \cdot \nabla \right) \mathbf{w} = -\nabla \tilde{p} + \mu_n \left(1 + \frac{3}{2} \varphi \sigma \right) \nabla^2 \mathbf{w} \quad (18)$$

For the incompressible flow as a result of the rotating plate, Eq. (18) and Eq.(4) have been converted into three-dimensional cylindrical form as:

$$-\frac{1}{\rho_n} \frac{\partial \tilde{p}}{\partial r} + \nu_n \left(1 + \frac{3}{2} \varphi \sigma \right) \left[\frac{\partial^2 w_r}{\partial r^2} + \frac{\partial}{\partial r} \left(\frac{w_r}{r} \right) + \frac{\partial^2 w_r}{\partial z^2} \right] = \left[w_r \frac{\partial w_r}{\partial r} + v_z \frac{\partial w_r}{\partial z} - \frac{w_\theta^2}{r} \right] \quad (19)$$

$$\nu_n \left(1 + \frac{3}{2} \varphi \sigma \right) \left[\frac{\partial^2 w_\theta}{\partial r^2} + \frac{\partial}{\partial r} \left(\frac{w_\theta}{r} \right) + \frac{\partial^2 w_\theta}{\partial z^2} \right] = \left[w_r \frac{\partial w_\theta}{\partial r} + w_z \frac{\partial w_\theta}{\partial z} + \frac{w_r w_\theta}{r} \right] \quad (20)$$

$$\frac{\partial w_r}{\partial r} + \frac{w_r}{r} + \frac{\partial w_z}{\partial z} = 0 \quad (21)$$

Subject to the boundary conditions:

$$\begin{aligned} z = 0; \quad w_r = 0, \quad w_\theta = r\omega, \quad w_z = 0; \\ z \rightarrow \infty; \quad w_r = 0, \quad w_\theta = 0 \end{aligned} \quad (22)$$

Density(ρ_n) and viscosity(μ_n) of nanofluid are

$$\rho_n = (1 - \varphi) \rho_f + \varphi \rho_s, \quad \mu_n = \frac{\mu_f}{(1 - \varphi)^{2.5}} \quad (23)$$

The following transformation is used to convert the given system into the dimensionless form:

$$\begin{aligned} w_r = r\omega E(\beta), \quad w_\theta = r\omega F(\beta), \quad w_z = \\ \sqrt{\nu \omega} G(\beta), \quad \tilde{p} = \rho \omega \nu P(\beta); \quad \beta = z \sqrt{\frac{\omega}{\nu}} \end{aligned} \quad (24)$$

From Eqs. (19)-(23) and by applying Eq. (24), the transformed nonlinear differential equations are as follows:

$$\begin{aligned} \left(1 + \frac{3}{2} \varphi \sigma \right) \left[\frac{1}{(1 - \varphi)^{2.5} \left(1 - \varphi + \varphi \frac{\rho_s}{\rho_f} \right)} \right] E''(\beta) - \\ G(\beta) E'(\beta) - E^2(\beta) + F^2(\beta) = 0 \end{aligned} \quad (25)$$

$$\begin{aligned} \left(1 + \frac{3}{2} \varphi \sigma \right) \left[\frac{1}{(1 - \varphi)^{2.5} \left(1 - \varphi + \varphi \frac{\rho_s}{\rho_f} \right)} \right] F''(\beta) - \\ G(\beta) F'(\beta) - 2E(\beta) F(\beta) = 0 \end{aligned} \quad (26)$$

$$G'(\beta) + 2E(\beta) = 0 \quad (27)$$

$$\begin{aligned} E(0) = 0, F(0) = 1, G(0) = 0, \\ E(\infty) = 0, F(\infty) = 0 \end{aligned} \quad (28)$$

3 Problem Solution

In the framework of this study, the nonlinear-coupled differential equations have been obtained for the flow of Fe_2O_3 water-based nanofluid owing to a rotating plate subject to the availability of an oscillating magnetic field. The set of nonlinear differential equations has been converted into solved with the help of COMSOL Multiphysics Software. Finally, the results have been obtained for the radial, azimuthal, and axial velocity profiles. The densities of the carrier liquid (ρ_f) and Fe_3O_4 nano-particles (ρ_s) are 1024 kg/m^3 and 5170 kg/m^3 , respectively. Figure 2 demonstrates the convergence plot of the numerical solution. The results in the numerical solution are corrected up to six decimal places. If we consider the parameters $\varphi = 0$ and $\sigma = 0$, the present problem reduces to Karman Swirling flow problems, [37], [38], [39]. In this case, Table 1 represents the validation of the present numerical solution with the previous theoretical model of Karman flow.

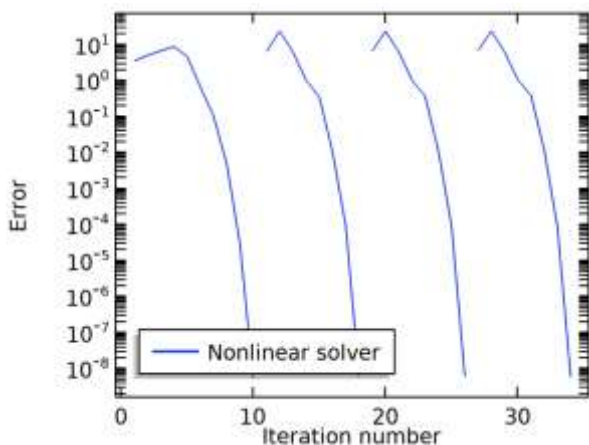


Fig. 2: Convergence plot of the numerical solution

Table 1. Validation of the numerical solution

	$E'(0)$	$F'(0)$
Kelson and Desseaux, [37]	0.510233	-0.65922
Pop et al., [38]	0.5102	-0.6159
Turkyilmazoglu [39]	0.5102326 2	- 0.61592201
Present Result	0.5102134 911	- 0.61590974 66

The authors are required to look over and verify whether the in-text citations exist in the reference list and whether all the references mentioned in the reference list exist in the in-text citations.

Also, they need to look over if the in-text citations of the Tables, Equations and Figures are

properly connected with the Tables, Equations and Figures.

4 Results and Discussion

Figure 3, Figure 4, and Figure 5 reveal the profiles of E, F , and G for various values of σ . In the absence of an effective magnetic parameter σ there is no magnetic torque acting on the fluid. Increasing the values of the parameter σ , the magnetic torque favors the swirling flow of Fe_2O_3 ferrofluid. The higher range of σ increases the velocity distributions. The Minus range of the axial velocity points out that the flow of nanofluid is oriented toward the plate. In Karman swirling flow, the velocities of ferrofluid are higher due to magnetic torque. Figure 6, Figure 7 and Figure 8 shows the distributions of E, F , and G for different sizes of volume concentrations of φ . Increasing the volume concentration of Fe_2O_3 decreases the velocity distribution in the flow increases. As we increase the concentration, the fluid becomes more magnetized. Therefore, the magnetic torque dominates over the flow which causes a significant enhancement in the velocity profiles. The results for $\varphi = 0$ indicate that only the flow of carrier liquid. With increasing values φ the magnetic fluid becomes magnetized and changes its behavior under the influence of the field. Figure 9, Figure 10 and Figure 11 exhibit the profiles of E, F , and G for different types of varieties of ferrofluids. The comparison has been made among $COFe_2O_4$, Fe_2O_3 , NiO , and CO nano-particles in a carrier liquid. The densities considered for these particles are 3594 kg/m^3 , 5170 kg/m^3 , 6670 kg/m^3 and 8860 kg/m^3 , respectively. The velocity of the ferrofluid depends on the types of nanoparticles and the carrier liquid. The velocity of the water-based CO ferrofluid is less than other nanofluids. The flow characteristics of ferrofluid can be controlled by changing the strength of the magnetic field as well as changing the ferromagnetic material.

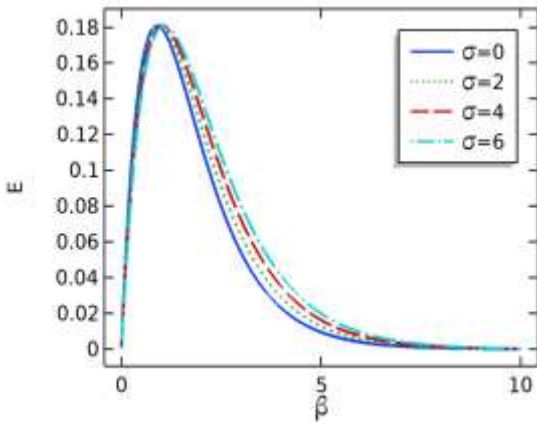


Fig. 3: Profile of E for different values of σ and fixed value of $\varphi = 0.05$

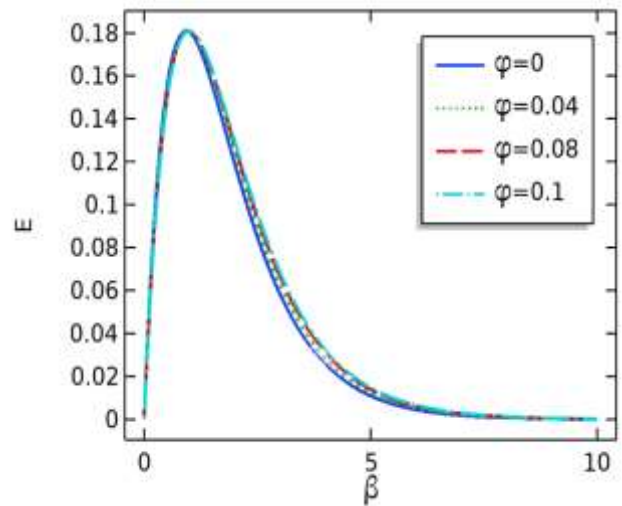


Fig. 6: Profile of E for different values of φ and fixed value of $\sigma = 2$.

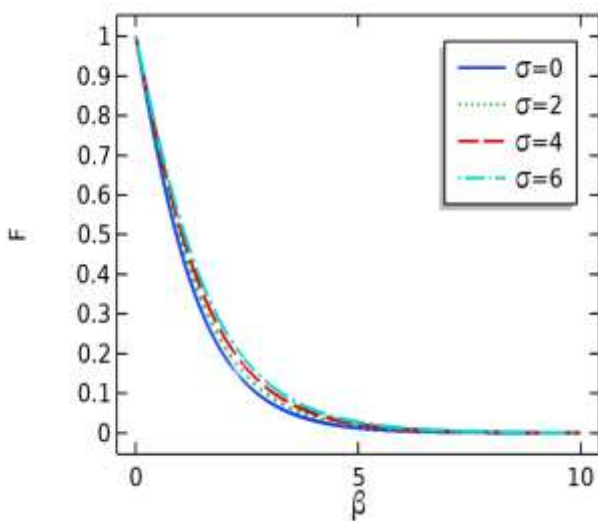


Fig. 4: Profile of F for different values of σ and fixed value of $\varphi = 0.05$

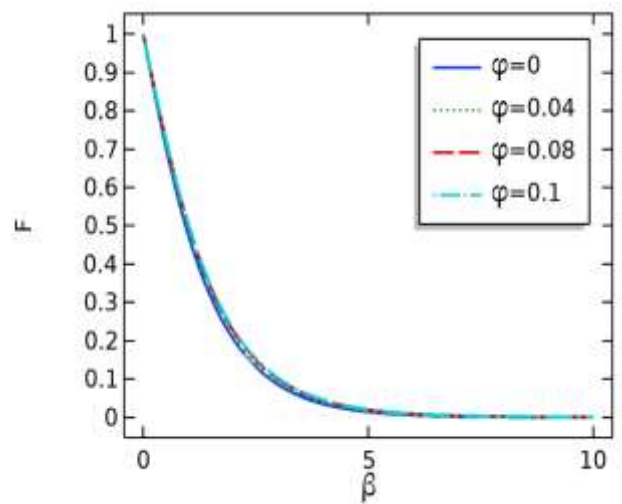


Fig. 7: Profile of F for different values of φ and fixed value of $\sigma = 2$.

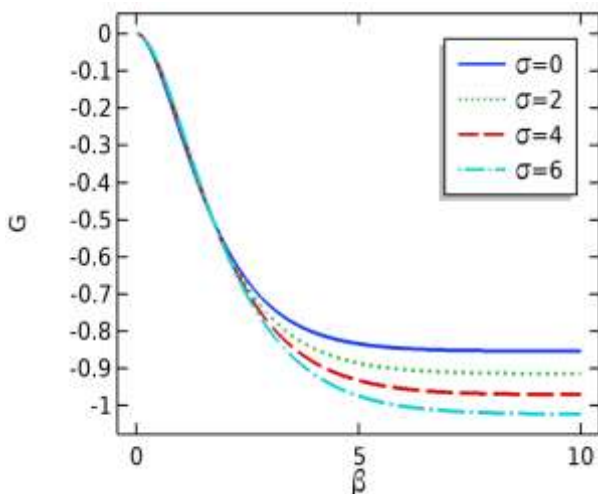


Fig. 5: Profile of G for different values of σ and fixed value of $\varphi = 0.05$

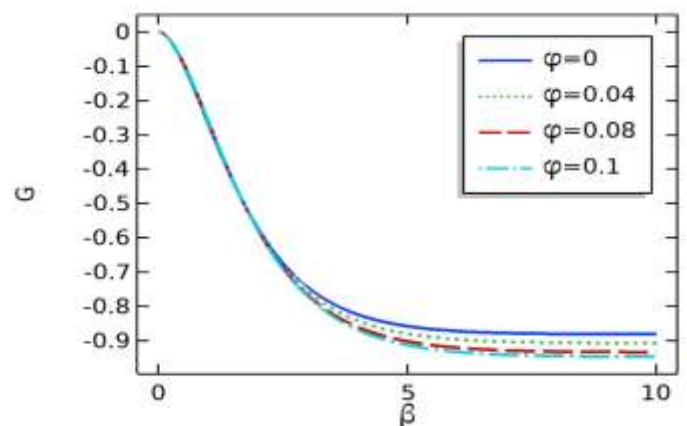


Fig. 8: Profile of G for different values of φ and fixed values of $\sigma = 2$

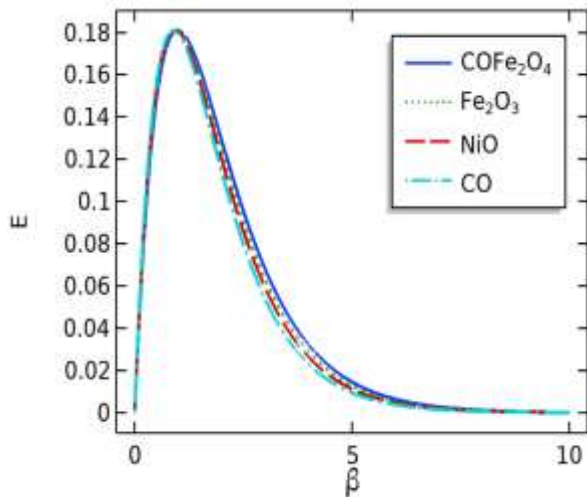


Fig. 9: Profile of E for different ferromagnetic nanoparticles

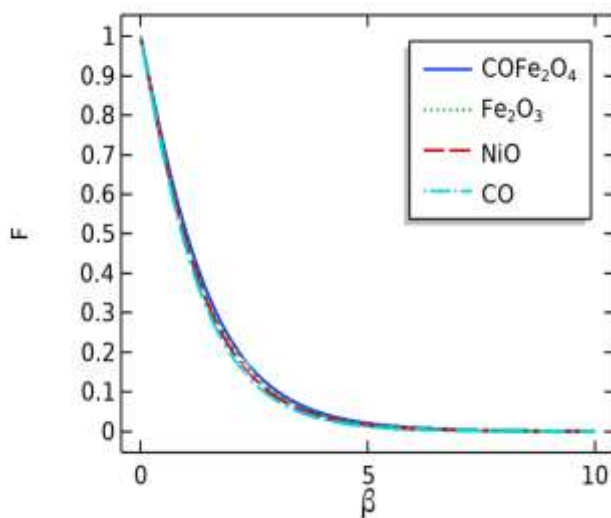


Fig. 10: Profile of F for different ferromagnetic nanoparticles

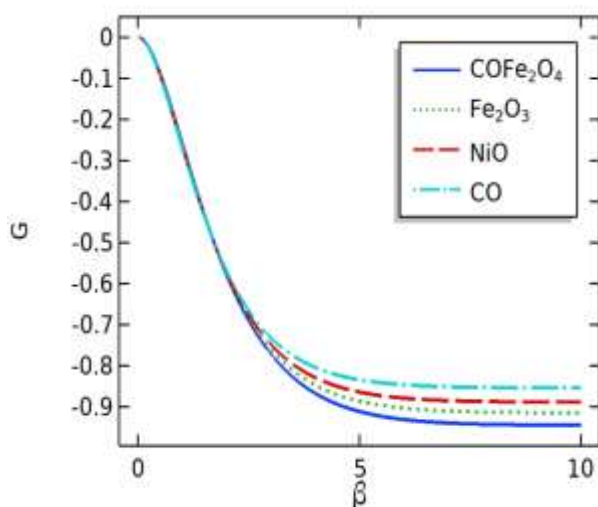


Fig. 11: Profile of G for different ferromagnetic nanoparticles

5 Conclusion

In this investigation, the outcome of ferromagnetic nanofluid flow over a rotating plate under the influence of the oscillating magnetic field has been studied numerically with the help of the finite element method. The main results of the present investigations are as follows:

- Growing volume concentration(φ) and effective magnetic parameter(σ) increases the velocity distributions in the flow.
- Water based Cobalt ferrite (COFe_2O_4) ferrofluid can be used as low viscous nanofluid and Cobalt (CO) ferrofluid can be used as a highly viscous nanofluid.
- These results could be useful for studying the rheological behavior of ferrofluids under the influence of the oscillating magnetic field.

References:

- [1] C. Rinaldi, A. Chaves, S. Elborai, X. He, and M. Zahn, Magnetic fluid rheology and flows, *Current Opinion in Colloid and Interface Science*, vol. 10, 2005, 141–157.
- [2] S. Genc and B. Derin, Synthesis and rheology of ferrofluids: A review, *Curr. Opin. Chem. Eng.*, vol. 3, 2014, 118–124.
- [3] R. E. Rosensweig, *Ferrohydrodynamics*, Cambridge University Press, New York, U.S.A., 1985.
- [4] S. Odenbach and S. Thurm, *Magnetoviscous Effects in Ferrofluids*, Springer Berlin, vol. 594, 2002, 185–201.
- [5] E. Blums, A. Cebers, M. M. Maiorov, *Magnetic Fluids*, Walter de Gruyter, U.K., 1997.
- [6] P. Ram and A. Bhandari, Effect of phase difference between highly oscillating magnetic field and magnetization on the unsteady ferrofluid flow due to a rotating disk, *Results Phys.*, vol. 3, 2013, 55–60.
- [7] P. Ram, A. Bhandari, and K. Sharma, Effect of magnetic field-dependent viscosity on revolving ferrofluid, *J. Magn. Magn. Mater.*, vol. 322, 2010, pp. 3476–3480.
- [8] R. Ravaut, G. Lemarquand, and V. Lemarquand, Mechanical properties of ferrofluid applications: Centering effect and capacity of a seal, *Tribol. Int.*, vol. 43, 2010, pp. 76–82.
- [9] J. Nowak, D. Wolf, and S. Odenbach, A rheological and microscopical characterization of biocompatible ferrofluids,

- J. Magn. Magn. Mater.*, vol. 354, 2014, pp. 98–104.
- [10] R. Patel, R. V. Upadhyay, and R. V. Mehta, Viscosity measurements of a ferrofluid: Comparison with various hydrodynamic equations, *J. Colloid Interface Sci.*, vol. 263, 2003, pp. 661–664.
- [11] F. M. Ali, R. Nazar, and N. M. Arifin, MHD Viscous Flow and Heat Transfer Induced by a Permeable Shrinking Sheet with Prescribed Surface Heat Flux, *WSEAS Trans. Math.*, vol. 9, 2010, pp. 365–375.
- [12] P. Roja, T. S. Reddy, S. M. Ibrahim, and G. Lorenzini, Analysis of Thermal radiation effects on MHD flow of a nanofluid over an exponentially stretching sheet with heat and mass fluxes in the occurrence of viscous dissipation, *WSEAS Trans. HEAT MASS Transf.*, vol. 17, 2022, pp. 141–150.
- [13] H. A. Ibrahim, M. G., asfour, Technical Simulation for the Hydromagnetic Rotating Flow of Carreau Fluid with Arrhenius Energy and Entropy Generation Effects: Semi-Numerical Calculations, *WSEAS Trans. FLUID Mech.*, vol. 17, 2022, pp. 229–240.
- [14] P. D. Ariel, “On computation of MHD flow near a rotating disk, *ZAMM Zeitschrift fur Angew. Math. und Mech.*, vol. 82, 2002, pp. 235–246.
- [15] J. Ahmed, M. Khan, L. Ahmad, A. K. Alzahrani, and M. Alghamdi, Thermally radiative flow of Maxwell nanofluid over a permeable rotating disk, *Phys. Scr.*, vol. 94, 2019, pp. 125016.
- [16] P. Sibanda and O. D. Makinde, On steady MHD flow and heat transfer past a rotating disk in a porous medium with ohmic heating and viscous dissipation, *Int. J. Numer. Methods Heat Fluid Flow*, vol. 20, 2010, pp. 269–285.
- [17] H. A. Attia, Unsteady MHD flow near a rotating porous disk with uniform suction or injection, *Fluid Dyn. Res.*, vol. 23, 1998, pp. 283–290.
- [18] N. Andhariya, B. Chudasama, R. Patel, R.V. Upadhyay, R.V. Mehta, Field induced rotational viscosity of ferrofluid: Effect of capillary size and magnetic field direction, *J. Colloid Interface Sci.*, vol. 323, 2008, pp. 153–157.
- [19] A. Y. Zubarev and L. Y. Iskakova, Rheological properties of ferrofluids with microstructures, *J. Phys. Condens. Matter*, vol. 18, 2006, pp. S2771–S2784.
- [20] M. I. Shliomis and K. I. Morozov, Negative viscosity of ferrofluid under alternating magnetic field, *Phys. Fluids*, vol. 6, 1994, pp. 2855–2861.
- [21] J. C. Bacri, R. Perzynski, M. I. Shliomis, and G. I. Burde, Negative-viscosity effect in a magnetic fluid, *Phys. Rev. Lett.*, vol. 75, 1995, pp. 2128–2131.
- [22] M. I. Shliomis, Ferrohydrodynamics: Testing a third magnetization equation, *Phys. Rev. E*, vol. 64, 2001, pp. 060501.
- [23] A. J. Chamkha and A. M. Aly, MHD free convection flow of a nanofluid past a vertical plate in the presence of heat generation or absorption effects, *Chem. Eng. Commun.*, vol. 198, 2010, pp. 425–441.
- [24] A. Bhandari and V. Kumar, Effect of magnetization force on ferrofluid flow due to a rotating disk in the presence of an external magnetic field, *Eur. Phys. J. Plus*, vol. 130, 2015, pp. 62.
- [25] Mustafa Turkyilmazoglu, MHD fluid flow and heat transfer due to a stretching rotating disk, *International journal of thermal sciences*, vol. 51, 2012, pp. 195–201.
- [26] A. Bhandari, Study of ferrofluid flow in a rotating system through mathematical modeling, *Math. Comput. Simul.*, vol. 178, 2020, pp. 290–306.
- [27] Mustafa Turkyilmazoglu, Effects of uniform radial electric field on the MHD heat and fluid flow due to a rotating disk, *International Journal of Engineering Science*, vol. 51, 2012, pp. 233–240.
- [28] M. Hassan, C. Fetecau, A. Majeed, and A. Zeeshan, Effects of iron nanoparticles’ shape on the convective flow of ferrofluid under highly oscillating magnetic field over the stretchable rotating disk, *J. Magn. Magn. Mater.*, vol. 465, 2018, pp. 531–539.
- [29] E. Shojaeizadeh, F. Veysi, K. Goudarzi, and M. Feyzi, Magnetoviscous effect investigation of water-based Mn-Zn Fe₂O₄ magnetic nanofluid under the influence of magnetic field: An experimental study, *J. Magn. Magn. Mater.*, vol. 477, 2019, pp. 292–306.
- [30] A. P. Krekhov, M. I. Shliomis, and S. Kamiyama, Ferrofluid pipe flow in an oscillating magnetic field, *Phys. Fluids*, vol. 17, 2005, pp. 033105.
- [31] B. Jalili, S. Sadighi, P. Jalili, and D. D. Ganji, Characteristics of ferrofluid flow over a stretching sheet with suction and injection, *Case Stud. Therm. Eng.*, vol. 14, 2019, pp.

- 100470.
- [32] S. A. M. Mehryan, E. Izadpanahi, M. Ghalambaz, and A. J. Chamkha, Mixed convection flow caused by an oscillating cylinder in a square cavity filled with Cu–Al₂O₃/water hybrid nanofluid, *J. Therm. Anal. Calorim.*, vol. 137, 2019, pp. 965–982.
- [33] D. Toghraie, R. Mashayekhi, H. Arasteh, S. Sheykhi, M. Niknejadi, and A. J. Chamkha, Two-phase investigation of water–Al₂O₃ nanofluid in a micro concentric annulus under non-uniform heat flux boundary conditions, *Int. J. Numer. Methods Heat Fluid Flow*, vol. 30, 2019, pp. 1795–1814.
- [34] E. Khodabandeh, D. Toghraie, A. Chamkha, R. Mashayekhi, O. Akbari, and S. A. Rozati, Energy saving with using of elliptic pillows in turbulent flow of two-phase water–silver nanofluid in a spiral heat exchanger, *Int. J. Numer. Methods Heat Fluid Flow*, vol. 30, 2019, pp. 2025–2049.
- [35] T. Tayebi and A. J. Chamkha, Entropy generation analysis during MHD natural convection flow of hybrid nanofluid in a square cavity containing a corrugated conducting block, *Int. J. Numer. Methods Heat Fluid Flow*, vol. 30, 2019, pp. 1115–1136.
- [36] Y. Menni, A. J. Chamkha, N. Massarotti, H. Ameer, N. Kaid, and M. Bensafi, Hydrodynamic and thermal analysis of water, ethylene glycol, and water–ethylene glycol as base fluids dispersed by aluminum oxide nano-sized solid particles, *Int. J. Numer. Methods Heat Fluid Flow*, vol. 30, 2020, pp. 4349–4386.
- [37] N. Kelson and A. Desseaux, Note on porous rotating disk flow, *ANZIAM J.*, vol. 42, 2000 pp. c837–c855.
- [38] N. Bachok, A. Ishak, and I. Pop, Flow and heat transfer over a rotating porous disk in a nanofluid, *Phys. B Phys. Condens. Matter*, vol. 406, 2011, pp. 1767–1772.
- [39] M. Turkyilmazoglu, Nanofluid flow, and heat transfer due to a rotating disk, *Comput. Fluids*, vol. 94, 2014, pp. 139–146.

Contribution of Individual Authors to the Creation of a Scientific Article (Ghostwriting Policy)

The authors equally contributed to the present research, at all stages from the formulation of the problem to the final findings and solution.

Sources of Funding for Research Presented in a Scientific Article or Scientific Article Itself

No funding was received for conducting this study.

Conflict of Interest

The authors have no conflicts of interest to declare.

Creative Commons Attribution License 4.0 (Attribution 4.0 International, CC BY 4.0)

This article is published under the terms of the Creative Commons Attribution License 4.0

https://creativecommons.org/licenses/by/4.0/deed.en_US